LA-UR -85-2840

CONF-850610--4

OSTI

SEP 1 0 1985

TITLE SCATTERING OF ELASTIC WAVES BY SMALL SURFACE-BREAKING OR SUBSURFACE CRACKS IN THREE DIMENSIONS

LA-UR--85-2840

DE85 017564

AUTHOR(S) William M. Visscher

SUBMITTED TO The Proceedings for the meeting "Review of Progress in Nondestructive Evaluation," held in Williamsburg, VA, June 24-28, 1985.

Los Alamos Los Alamos National Laboratory
Los Alamos, New Mexico 87545

SCATTERING OF ELASTIC WAVES BY SMALL SURFACE-BREAKING OR SUBSURFACE CRACKS IN THREE DIMENSIONS

William M. Visscher†

Theoretical Division, MS-B262
Los Alamos National Laboratory
Los Alamos, NM 87545

ABSTRACT

The long-wavelength limit of elastic wave scattering by surface cracks in 3d is considered. It is shown that, if the crack is normal to the surface, the scattering can be described by two real parameters, one of which may be taken to be the crack size. The other therefore depends on shape, orientation, and burial depth. Many computed illustrations are given. It is concluded that the amount of information about cracks obtainable by low frequency elastic wave scattering is very limited.

INTRODUCTION

Dangerous cracks (those which cause failures) usually start on surfaces, and are initially small. Thus ultrasonic detection in early stages of crack growth is always in the regime where wavelength is large compared to the crack dimensions. It is therefore of special interest to consider what can be learned about the size and shape of small cracks on or near surfaces by scattering elastic waves from them.

It may be that even at long wavelengths, where scattering is bound to be simple as far as angular distribution is concerned, some cracks will exhibit a signature which identifies them as dangerous fast-growing cracks while others can be ignored as benign.

This paper addresses the question of exactly what features of crack geometry can be identified by long-wavelength elastic wave scattering.

In order to simplify the analysis the cracks are assumed (this assumption can be checked from scattering data) to be flat and to be oriented perpendicular to the free surface, which is assumed to be infinite and planar.

There are, of course, no practical situations in which these conditions are fully realized, but our results may give some insight into the potential utility and limitations of such methods.

† Supported by the DOE

The plan of this paper is first to review the situation for cracks in bulk for long wavelength scattering, and then to consider the case of cracks on or near free plane surfaces.

THE SCATTERED AMPLITUDE

A. An isolated crack

It has been shown many times that the amplitude for scattering from an isolated crack is a linear functional of the crack-opening-displacement (COD) $\Delta\vec{u}(\vec{r})$ [1,2,3];

$$f(\pi,\hat{\gamma},\pi^0,\hat{\gamma}_0) = F(\omega) \int_c ds\vec{\tau}^{\pi^\dagger}(\hat{\gamma},\vec{r})\cdot\vec{\Delta}u(\vec{r}) \quad , \tag{1}$$

where $\pi,\hat{\gamma},\pi^0,\hat{\gamma}_0$ are polarizations (π = SH,SV,P) and directions ($\hat{\gamma}\cdot\hat{\gamma} = 1$) of incident plane waves $(\pi^0,\hat{\gamma}_0)$ and of observation $(\pi,\hat{\gamma})$. $\vec{\tau}^{\pi}(\hat{\gamma},\vec{r})$ is the traction at the crack surface (in the absence of the crack) associated with a plane wave in the direction $\hat{\gamma}$ with polarization π and frequency ω. The integral is on the "top" surface of the crack, where $\vec{\Delta}u = \vec{u}^{\text{"top"}} - \vec{u}^{\text{"bottom"}}$.

If the crack is assumed to include the origin, and we restrict ourselves to the limit where $kL \ll 1$ (L is a characteristic dimension of the crack, and k is the shear wavenumber), then Eq. (2) becomes

$$f(\pi,\hat{\gamma},\pi^0,\hat{\gamma}_0) = F(\omega)A\vec{\tau}^{\pi^\dagger}(\hat{\gamma})\cdot\overline{\Delta u} \quad , \tag{2}$$

where A is the crack area, $\vec{\tau}^{\pi}(\hat{\gamma}) = \vec{\tau}^{\pi}(\hat{\gamma},0)$, and $\overline{\Delta u}$ is the COD averaged over the crack surface C.

It is intuitively reasonable, and it can be shown quite easily, that the COD, too, is a linear functional of the asymptotic stresses; in particular, it is a linear functional of the tractions at the crack surface, which would be present if the crack weren't, associated with the incident displacement field. In the Rayleigh limit the algebraic expression of this statement is

$$\overline{\Delta u} = X\vec{\tau}^{\pi^0}(\hat{\gamma}_0) \tag{3}$$

where X is a 3×3 matrix, independent of π^0 and $\hat{\gamma}_0$.

It can be shown [2] (with some effort one can, from the symmetries of the situation, convince oneself that it is true) that, if the crack is, say, in the yz plane,

$$X = \begin{bmatrix} X_{xx} & 0 & 0 \\ 0 & X_{yy} & X_{yz} \\ 0 & X_{zy} & X_{zz} \end{bmatrix} \quad . \tag{4}$$

Using Eqs. (2), (3) and (4), and the reciprocity requirement [4]

$$f(\pi,\hat{\gamma},\pi^0,\hat{\gamma}_0) = f(\pi^0,-\hat{\gamma}_0,\pi,-\hat{\gamma}) \tag{5}$$

a little simple algebra leads to the conclusion that Eq. (5) is satisfied if $X_{yz} = X_{zy}$. Detailed calculation verifies that this is the case.

The scattering from a small crack is therefore completely specified by 6 real numbers, X_{xx}, X_{yy}, X_{zz}, X_{yz}, and two angles which specify the angle of the crack plane relative to the yz plane. One of the four X_{ij}'s specifies the rotation of the crack in its plane, so that 3 real parameters remain to describe the size and shape of the crack. Calculations, using a particular parameterization of cross-sections, have been performed [2], leading to the conclusion that long-wavelength scattering measurements, even if performed with exceptional accuracy, will yield little information about crack shape; i.e. there is always a circular crack whose long-wavelength scattering is nearly the same as a crack of complicated shape.

B. The Surface Crack

The foregoing is the situation for the isolated crack. One may hope that the paucity of information available there might be improved by the presence of a free surface nearby which could amplify the effects of crack shape by multiple scattering.

The formulas for the surface crack are to a large extent identical to those for the bulk crack. Just some reinterpretation is necessary. For example, Eq. (1) still holds, with the possible values of π extended to include Rayleigh surface waves; viz. π = SH,SV,P, and R. The basic traction $\vec{\tau}^{\pi}(\hat{\gamma},\vec{r})$ for π = SH, SV, and P is a linear combination of up-and downgoing waves which satisfies the traction-free boundary condition at $z = 0$ (the free surface, with vacuum above it, is the xy plane); for π = R it is a linear combination of evanescent P and SV waves which is traction-free on the xy plane. (Explicit expressions can be found in Ref. 3).

Equations (2), (3), and (4) still hold for the surface crack, and so does Eq. (5) with the proviso that $\hat{\gamma}_0$ is upward-going and $\hat{\gamma}$ is downward-going for SH, SV, and P; they are both evanescent for π = R.

Scattering by small surface cracks is simplified compared to isolated cracks by the fact that now

$$\tau_z^{\pi}(\hat{\gamma},0) = \tau_z^{\pi}(\hat{\gamma}) = 0 \tag{6}$$

by construction; i.e. although $\vec{\tau}$ is a traction on the crack surface, τ_z is the x-component of the traction on the free surface (xy plane), because the crack (in the yz plane) is perpendicular to the free surface.

This means that the scattered amplitude from the surface crack is simpler than that for the bulk crack; using Eqs. (2), (3), (4), and (6), we get, dropping some superfluous (at present) normalizations

$$f(\pi,\hat{\gamma},\pi^0,\hat{\gamma}_0) = \tau_x^{\pi^\dagger}(\hat{\gamma})X_{xx}\tau_x^{\pi^0}(\hat{\gamma}_0) + \tau_y^{\pi^\dagger}(\hat{\gamma})X_{yy}\tau_y^{\pi^0}(\hat{\gamma}_0) \quad . \tag{7}$$

Scattering from a small surface-breaking (or near surface) crack is completely described, after its orientation is known, by just 2 parameters dependent on the size and shape of the crack.

The reduction in the number of determinable parameters X_{ij} from 4 in the case of the bulk crack to 2 in the case of the surface crack can be blamed on the presence of the free surface, which reduces the number of traction components with which we can probe from 3 to 2. Thus we should expect less information about the crack to be obtainable when there is a surface nearby than otherwise.

COMPUTED EXAMPLES

Equation (7), for $\pi = \pi^0 = R$, is

$$f(\pi,\hat{\gamma},\pi^0,\hat{\gamma}_0) = \alpha[(\cos^2\phi + \tfrac{1}{2})(\cos^2\phi_0 + \tfrac{1}{2}) + \beta \sin2\phi \sin2\phi_0] \quad , \tag{8}$$

where ϕ_0, ϕ are the incident and scattered azumuthal angles ($\phi_0 = 0$ is normal incidence) and Rayleigh surface waves are incident and scattered. This expression is obtained by substituting the expression for τ in Ref. 2 into Eq. (7); corresponding expressions can be written down for all π, π^0; always involving the same 2 parameters depending on crack geometry, which for convenience we have called α, β. The $\frac{1}{2}$'s which appear in Eq. (8) depend on the elastic material: we have taken Poisson's ratio to be 1/3.

If one measures the backscattering amplitude $f(\phi_0+\pi, \phi_0)$, then Eq. (8) says there is a maximum at $\phi_0 = 0$, (normal incidence), as one would expect, and a minimum at $\phi_0 = \pi/2$ (edge-on incidence), also as one might expect. The ratio of the two amplitudes

$$\frac{f(\pi,0)}{f(\frac{\pi}{2},-\frac{\pi}{2})} = 9 \tag{9}$$

is fixed for all flat cracks normal to the flat surface; if it is much different from 9 then either the crack is not flat or not normal to the surface.

So experimentally one can find the $\phi_0 = 0$ direction by seeking the maximum in backscattering, then one can verify flatness and normality by measuring $f(\pi/2,-\pi/2)$. If Eq. (9) is satisfied, then one can proceed to determine β by measuring one or more of a number of amplitudes with either or both ϕ and ϕ_0 equal to ± 45° or ± 135°. For example, the 45° backscattering amplitude is

$$\frac{f(-3\pi/4,\pi/4)}{f(\pi,0)} = \frac{1+\beta}{9/4} \quad , \tag{10}$$

and the 45° specular amplitude is

$$r = \frac{f(3\pi/4,\pi/4)}{f(-3\pi/4,\pi/4)} = \frac{1-\beta}{1+\beta} \quad , \tag{11}$$

or

$$\beta = \frac{1-r}{1+r} \quad . \tag{12}$$

β is the <u>only</u> parameter depending on the shape and orientation of the crack which can be obtained from long-wavelength scattering. α scales with the size of the crack and the incident wavenumber k

$$\alpha \propto L^3 k^{5/2} \tag{13}$$

(L is any dimension of the crack); thus if one increases all the dimensions of the crack (including its burial depth, if it is subsurface) by a factor g, then α increases by a factor g^3. (But if one simultaneously increases the wavelength by the same factor g, then α increases only by a factor $\sqrt{g}$.)

The figures which follow illustrate the dependence of α and β on the crack shape and situation relative to the free surface. The cross-sections have been computed using the CODE [3] (crack-opening-displacement-expansion) method, in which the COD is expanded in a set of gaussians centered on a square array of points on the crack surface. Most of the computation time is consumed calculating elements of a 3N × 3N matrix, where N is the number of localized gaussians. Once the matrix is computed, scattering from any crack which can be simulated by a subset of the points can be obtained, for any incident and scattered polarization and direction, without much further numerical work. We take N = 56, representing an array 8 deep (z-direction) and 7 wide (y-direction). The lattice spacing, a, merely supplies a scale factor. It has been established [5] that a surface-breaking crack is simulated if the top row of localized function has centers 0.65a below the free surface, and that the effective crack edge (for simple shapes) is 0.94a beyond the last row or column of lattice points. See Fig. 1.

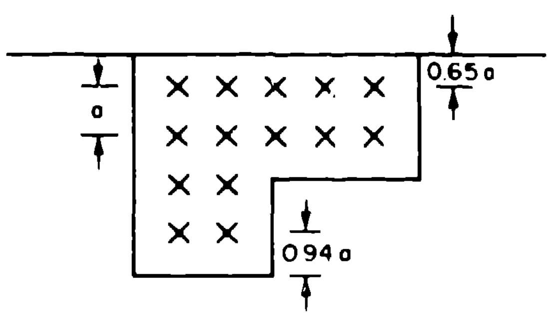

Fig. 1 A linear combination of gaussians centered on points in a square array is used to simulate the COD. It has been found [3] that surface-breaking cracks are simulated if the topmost centers are 0.65a below the free surface. The crack edge is about 0.94a beyond the last centers [2].

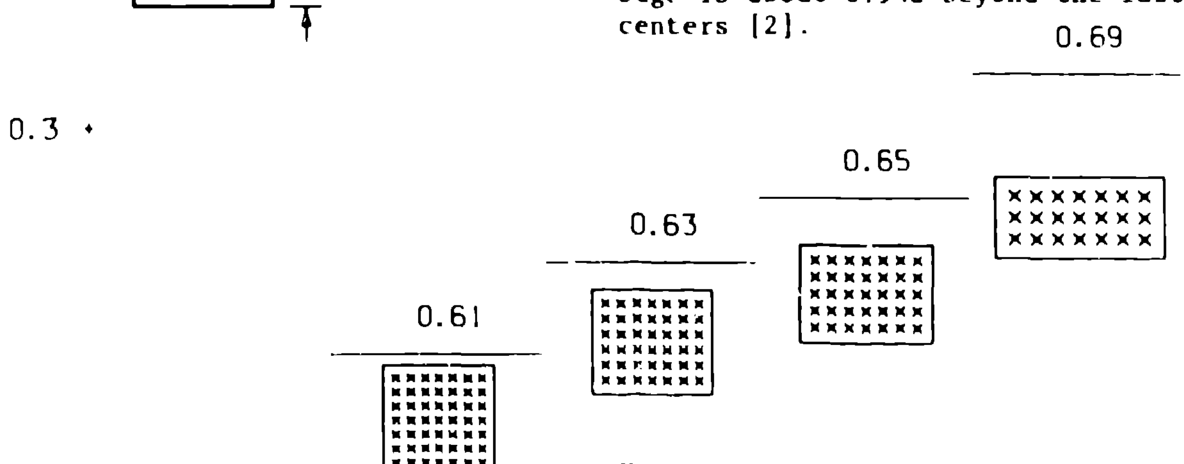

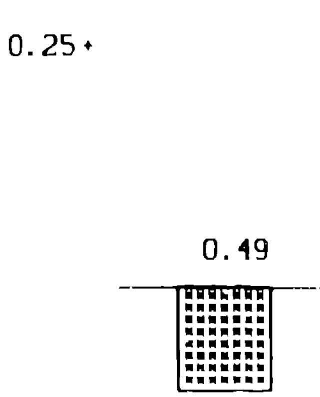

Fig. 2 A family of surface cracks. At the left is a 7 × 8 array of localized functions simulating a rectangular surface-breaking crack. The horizontal line represents the free surface. Successively deeper subsurface cracks are simulated by simply amotting more and more rows of localized functions. The height of the surface line is the value of β according to the scale at the left; the size of each drawing is adjusted so that all cracks on this and the following figures give the same normal backscatter. The numbers above the free surface lines are the crack areas in arbitrary units

Figures 2-8 give results of computing α and β for several families of surface-breaking and near-surface cracks. The cracks are scaled in the drawing so that the normal Rayleigh-Rayleigh backscatter from each is the same, and the vertical position of the line representing the position of the free surface is the value of β according to the scales at the left.

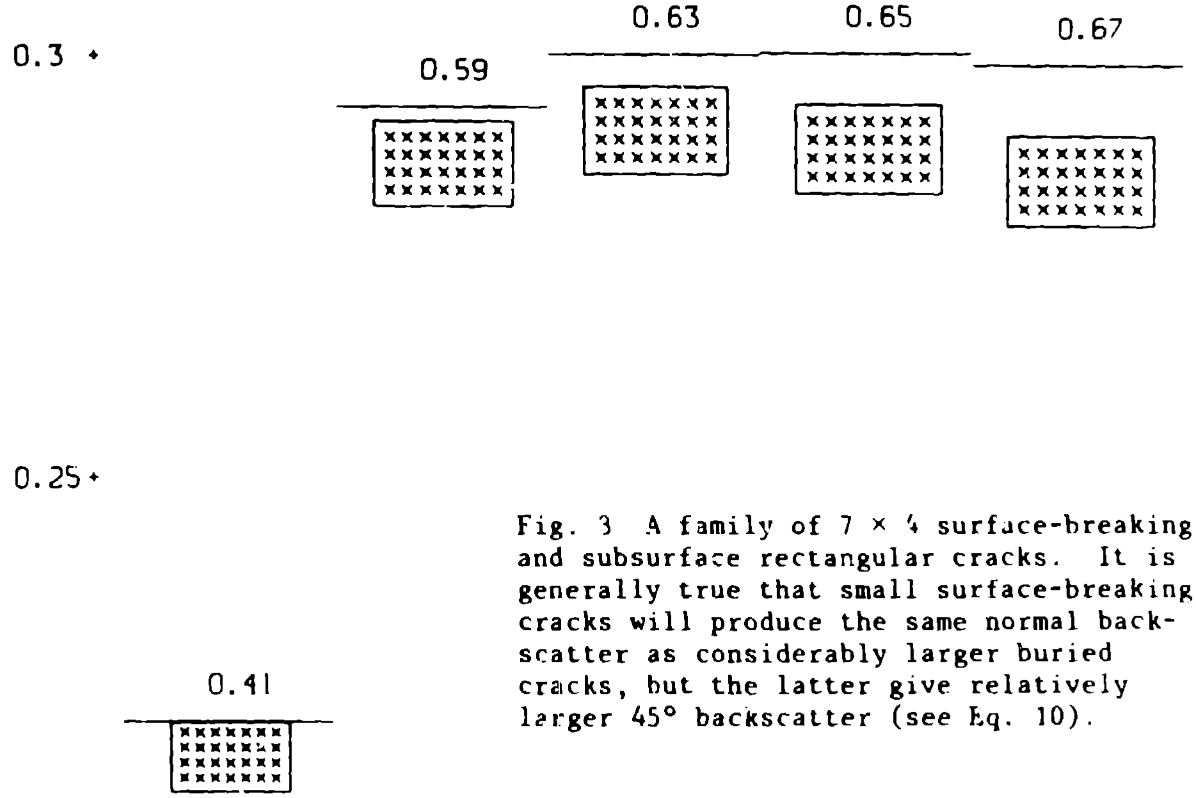

Fig. 3 A family of 7 × 4 surface-breaking and subsurface rectangular cracks. It is generally true that small surface-breaking cracks will produce the same normal backscatter as considerably larger buried cracks, but the latter give relatively larger 45° backscatter (see Eq. 10).

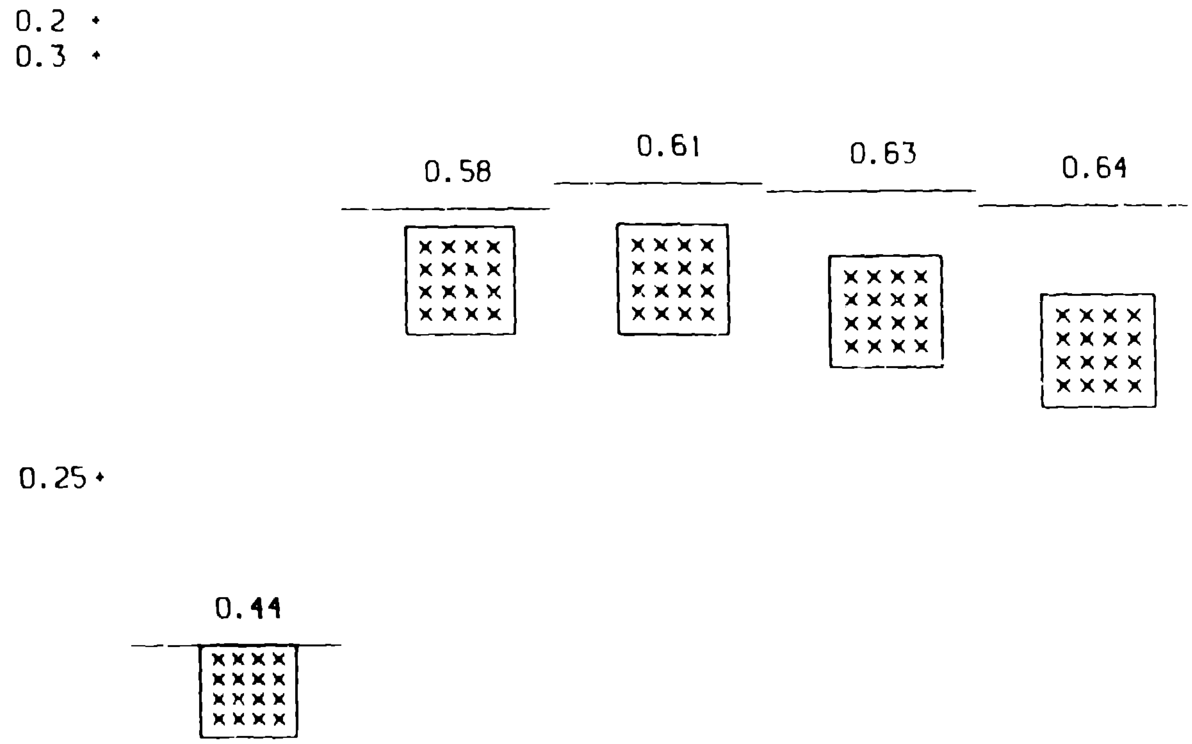

Fig 4. A set of square cracks. Experimentally these are probably indistinguishable from the rectangular cracks or the

0.25 +

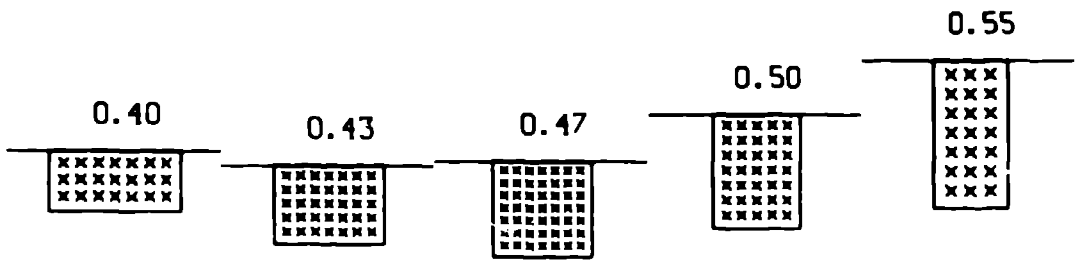

Figure 5 Rectangular cracks with different aspect ratios: 7 × 3, 7 × 5, 7 × 7, 5 × 7, 3 × 7.

0.2 +

0.3 +

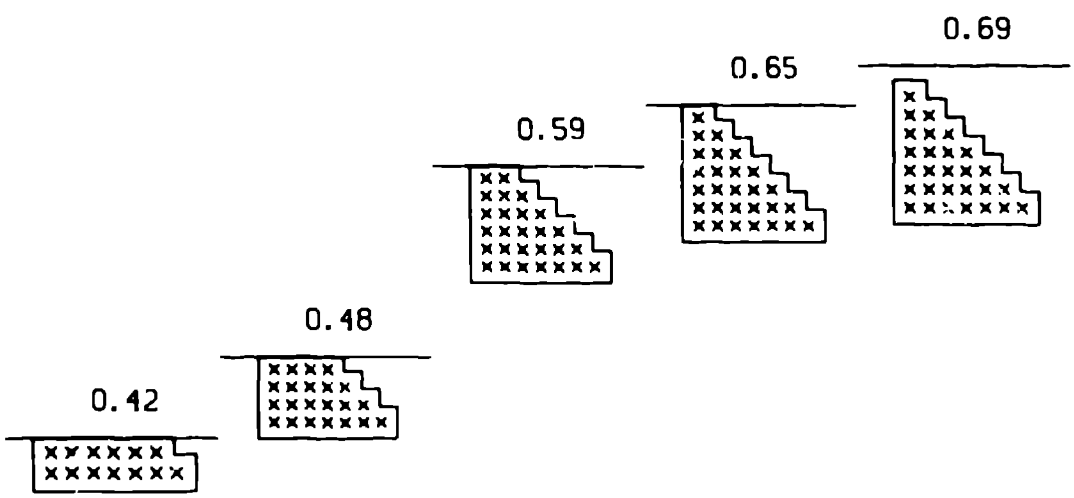

0.25 +

Fig. 6 A sequence of cracks which are truncated triangles. This supplies a continuous transition from surface-breaking to subsurface cracks.

0.2 +

DISCUSSION

The data contained in Figs. 5 and 7 and similar calculations can be analyzed to show that, to a good approximation, the scattered amplitude from rectangular surface-breaking cracks (and probably any surface-breaking crack whose maximum width is at the surface) is nearly proportional to ℓS, where ℓ is the width of the crack at the surface, and S is its area ($S = \ell d$, where d is the depth, for a rectangular crack). The relation is, for cracks with aspect ratio greater than 0.3,

$$A = \ell(S - 0.15\,\ell^2) \quad ,$$

where A is the normal Rayleigh-Rayleigh (RR) backscattering amplitude in arbitrary units. Equation (14) is consistent with measurements reported by Resch et al. [6]. So ℓS may be obtained from RR backscattering

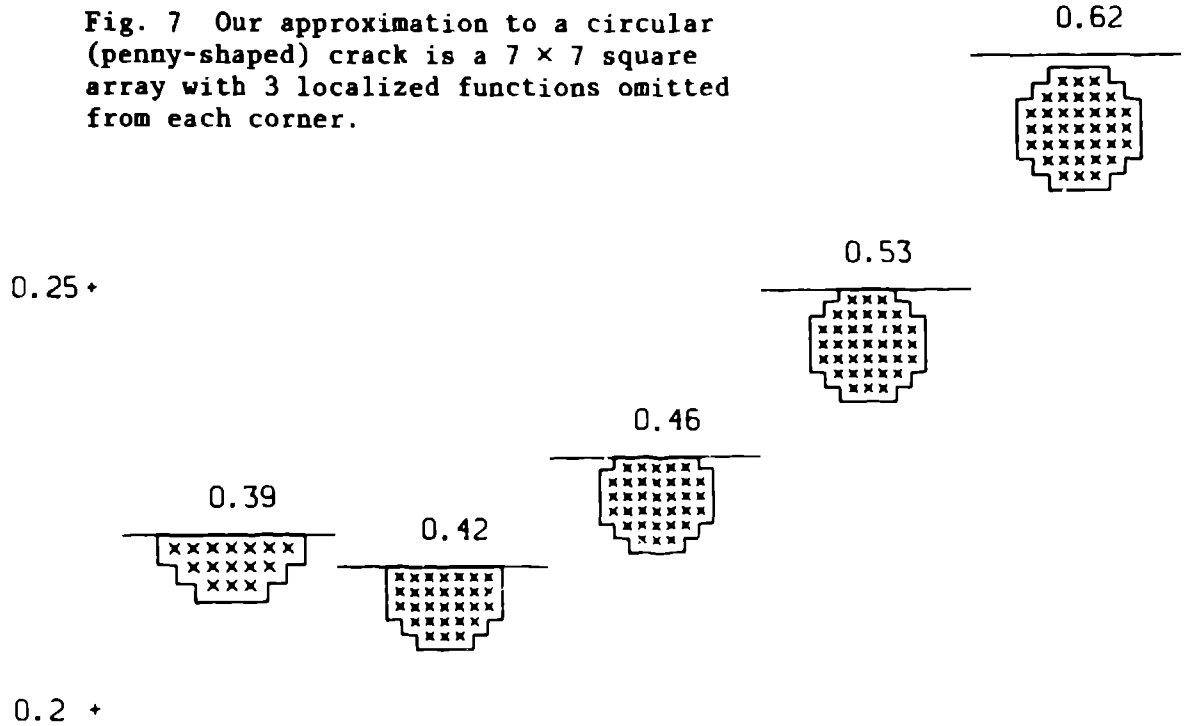

Fig. 7 Our approximation to a circular (penny-shaped) crack is a 7 × 7 square array with 3 localized functions omitted from each corner.

The angular distribution of RR backscatter (Eq. 13, with $\phi = \phi_0$) will yield β. Our calculations yield the result that β is essentially 2-valued, being 0.23 ± 0.01 for surface-breaking cracks and about 0.29 ± 0.01 for subsurface cracks, if Poisson's ration is 1/3. This agrees with the results of Auld [7], who wrote an expression for long-wavelength RR backscatter from a halfpenny surface-breaking crack assuming that the static COD was the same as the isolated penny-shaped crack.

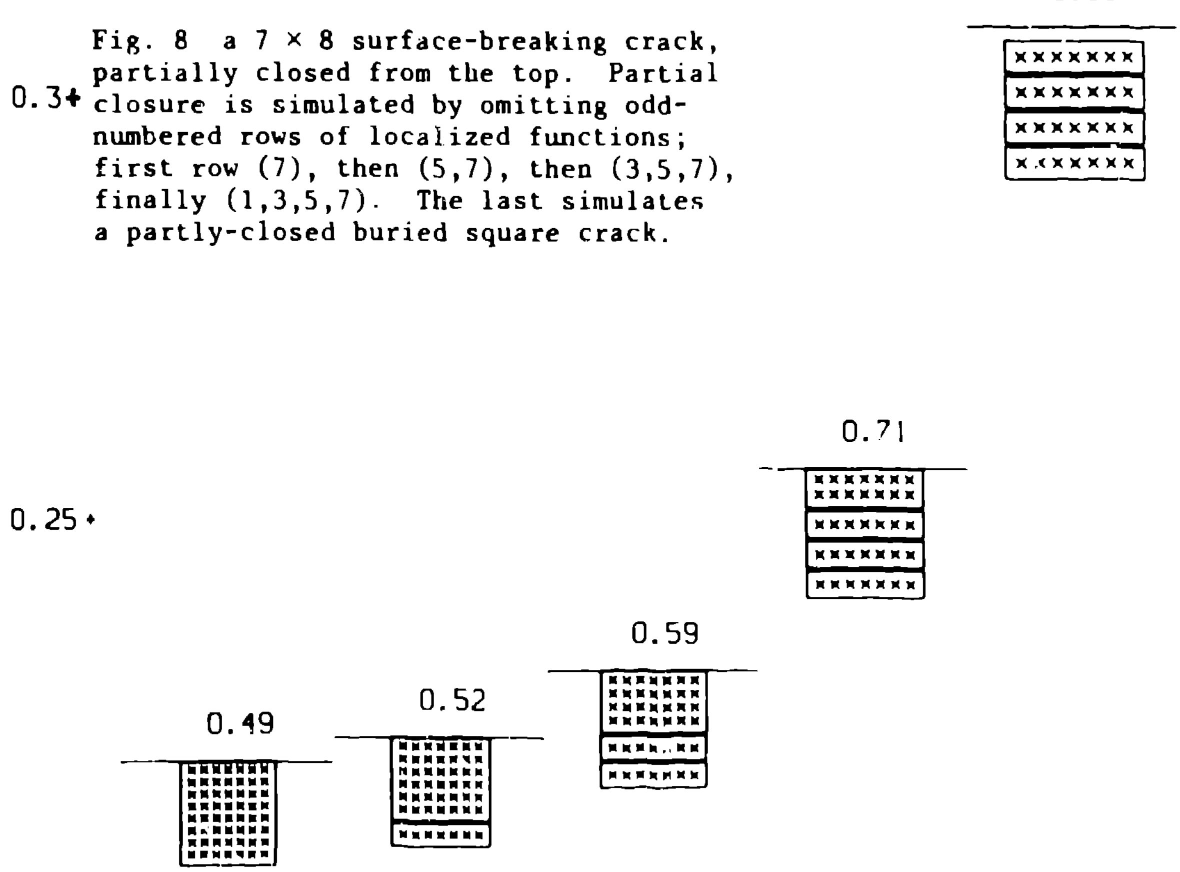

Fig. 8 a 7 × 8 surface-breaking crack, partially closed from the top. Partial closure is simulated by omitting odd-numbered rows of localized functions; first row (7), then (5,7), then (3,5,7), finally (1,3,5,7). The last simulates a partly-closed buried square crack.

More than routine accuracy may be needed to distinguish surface-breaking from subsurface cracks in this way. The ratio r = (45° RR specular)/(45° RR backscatter) is 0.63 for surface-breaking cracks, 0.55 for subsurface ones.

Another fact which can be gleaned from our calculations is that the scattering amplitude of a surface-breaking crack decreases by 40 or 50% if the crack is buried by an amount equal to its mutual depth. Most of the decrease occurs as soon as the burial starts, and the largest decrease is for high aspect-ratio cracks. Thus the only way to distinguish a small surface-breaking crack from a somewhat larger subsurface crack is by measuring β.

REFERENCES

1. J. E. Gubernatis, E. Domany, and J. A. Krumhansl, J. Appl. Phys. 48, 2804 (1973).
2. William M. Visscher, Wave Motion 5, 15 (1983).
3. William M. Visscher, J. Appl. Phys. 57, 1538 (1985).
4. William M. Visscher, J. Acoust. Soc. Ann. 69, 50 (1981).
5. William M. Visscher, J. Appl. Phys. 56, 713 (1984).
6. M. T. Resch, J. C. Shyne, G. S. Kino, and D. V. Nelson, Rev. of Prog. in Quantitative NDE, V.1 (Ed. D. O. Thompson and D. E. Chimenti) (Plenum, 1982) p. 573.
7. B. A. Auld, Wave Motion 1, 3 (1979).